Published in final edited form as:

Neurobiol Aging. 2015 May ; 36(5): 1834–1848. doi:10.1016/j.neurobiolaging.2015.02.001.

Normal-Appearing Cerebral White Matter in Healthy Adults: Mean Change over Two Years and Individual Differences in Change

Andrew R. Bender and

Institute of Gerontology, Wayne State University

Naftali Raz

Institute of Gerontology & Department of Psychology, Wayne State University

Abstract

Diffusion tensor imaging (DTI) studies show age-related differences in cerebral white matter (WM). However, few have studied WM changes over time, and none evaluated individual differences in change across a wide age range. Here, we examined two-year WM change in 96 healthy adults (baseline age 19-78 years), individual differences in change, and the influence of vascular and metabolic risk thereon. Fractional anisotropy (FA), axial diffusivity (AD) and radial diffusivity (RD) represented microstructural properties of normal appearing WM within 13 regions. Cross-sectional analyses revealed age-related differences in all WM indices across the regions. In contrast, latent change score analyses showed longitudinal declines in AD in association and projection fibers, and increases in anterior commissural fibers. FA and RD evidenced a less consistent pattern of change. Metabolic risk mediated the effects of age on FA and RD change in corpus callosum body and dorsal cingulum. These findings underscore the importance of longitudinal studies in evaluating individual differences in change, and the role of metabolic factors in shaping trajectories of brain aging.

Keywords

brain; aging; longitudinal; white matter; DTI; metabolic syndrome

*Corresponding author at: Max Planck Institute for Human Development, Lentzeallee 94, 14195 Berlin, Germany. Tel.: +49 30 82406 354; fax: +49 30 8249939..

Author Note

Andrew R. Bender, Institute of Gerontology, Wayne State University; Naftali Raz, Department of Psychology, Institute of Gerontology, Wayne State University.

Disclosure Statement The authors of this publication have no conflicts to disclose.

1. Introduction

Human brain structure changes with age, but the rate of change varies across brain regions and among individuals (see Kemper, 1994; Raz and Kennedy, 2009; Raz and Rodrigue, 2006 for reviews). The extant investigations of structural brain changes across time are limited mostly to gross neuroanatomy, and substantially less is known about age-related changes in other aspects of the brain. In particular, little is known about trajectories of changes in the microstructural organization of cerebral white matter (WM), reflected in local properties of water diffusion and evaluated mainly through diffusion tensor imaging (DTI; Beaulieu and Allen, 1994), and particularly little is known about individual differences in the rate of change.

The major obstacle to understanding age-related changes in WM is the scarcity of longitudinal studies. Whereas the cumulative record of cross-sectional DTI studies shows consistent age-related differences in multiple indices of WM microstructure across many brain regions (Madden et al., 2009, 2012), only a handful of studies have examined change across time in healthy adults, most within a limited age range (Barrick et al., 2010; Charlton et al., 2010; Sullivan et al., 2010; Teipel et al., 2010; Lövdén et al., 2014). Moreover, no prior longitudinal DTI study of the adult lifespan has examined individual differences in change and potential mediators thereof. Quantifying individual differences in change is an essential prerequisite for understanding factors contributing to differential age trajectories and sorting out normal and pathological processes in the life-span development of the brain.

Among multiple potential mediators of individual differences in brain aging, vascular risk factors may be especially promising. Vascular risk and metabolic dysregulation increase with age (Ervin, 2009) and contribute to cross-sectional age-related differences in DTI indices (Burgmans et al., 2010; Hannesdottir et al., 2009; Marks et al., 2011; Miralbell et al., 2012; O'Sullivan et al., 2005; Segura et al., 2009; Stanek et al., 2010; Vernooij et al., 2008; Williams et al., 2013; Xu et al., 2013). Furthermore, both age and vascular risk are associated with significant occurrence and progressive increase in white matter hyperintensities (WMH), structural discontinuities in the normal WM that reflect multiple neurobiological and neuropathological processes (e.g., Schmidt et al., 1999; Raz et al., 2012), and are associated both with vascular risk and reduced cognitive performance (DeCarli et al., 1995; Hunt et al., 1989; see Debette et al., 2011; Gunning-Dixon and Raz, 2000 for reviews). The presence of WMH alters magnetic resonance imaging (MRI) signal characteristics (Gouw et al., 2008) and DTI studies of aging populations that control for the influence of WMH on WM diffusion properties (Vernooij et al., 2008) reveal outcomes significantly different from the results produced by investigations that assessed total WM (Maillard et al., 2013).

Vascular risk is closely associated with deficits in many indicators of metabolic activity, and various combinations of vascular and metabolic risk factors are quite common in the general population. Moreover, the risk of vascular and metabolic dysregulation increases with age, and over 40% of North American adults over 60 years of age meet the criteria for metabolic syndrome (Ervin, 2009; Ford et al., 2002). Metabolic syndrome is characterized by increased abdominal adiposity, elevated blood pressure, dyslipidemia, and dysregulation of

glucose metabolism. Various indicators of metabolic and vascular risk have been linked to altered diffusion properties of WM (Bolzenius et al., 2013; Burgmans et al., 2010; Jacobs et al., 2013; Kennedy & Raz, 2009; Williams et al. 2013). Thus, metabolic risk factors may explain individual differences in WM change, and even studies of healthy aging samples should account for their possible influence.

It stands to reason that elucidation of brain aging depends on clarifying the patterns of change in multiple indices of cerebral organization and integrity over time, documenting individual differences in the rate of change, and gauging the role of important age-related factors in producing these differences. Cross-sectional age-comparative studies can show age-related differences and provide patterns of mean age-related change over a wide time window.

However, they reveal nothing about individual differences in change (Hofer et al., 2006; Lindenberger et al., 2011) and fail at establishing mediators of these differences (Maxwell and Cole, 2007), especially over relatively short periods. Unfortunately, not only are longitudinal studies of the brain's structural changes rare, but the most commonly used analytical procedures focus primarily on mean change and ignore individual variability in change. In response to this limitation of difference scores, paired t-tests, and traditional repeated measures, latent change score modeling (LCSM) techniques were developed to allow estimation of mean change and variance in change on the level of latent variables separately from measurement error at multiple occasions (McArdle and Nesselroade, 1994). Once variance in change is observed, incorporation of relevant covariates in LCSM provides an opportunity to evaluate variables that may explain these individual differences. LCSM analyses have been successfully applied to the study of age-related changes in brain structure, such as brain shrinkage and ventricular enlargement (see McArdle et al., 2004; Raz et al., 2005, 2008). These analytic techniques have only recently been used to investigate change in WM diffusion properties (Lövdén et al., 2014) in a narrow-age sample of very old adults, and no investigations to date have used such methods to evaluate WM change across the adult lifespan.

This study was designed to address some of the outlined concerns. First, we examined two-year change in regional diffusion properties of normally appearing WM in healthy volunteers across the adult life span. Second, by applying the LCSM analytic approach, we evaluated individual differences in change and examined advanced age and vascular risk as modifiers of that variability. Third, we examined the role of indicators of risk for metabolic syndrome as potential mediators of the effects of age on longitudinal change in WM.

2. Methods

2.1. Participants

All participants were recruited from the greater Detroit, Michigan metropolitan area through advertisements in local newspapers and flyers for a longitudinal investigation of brain and cognitive aging. Cross-sectional age differences in coarsely defined regions of WM in the middle- and older-aged part of this sample have been previously reported (Burgmans et al., 2010). At both measurement occasions, participants provided informed consent in accord

with the University Institutional Review Board guidelines and completed a detailed health questionnaire to screen for history of neurological and psychiatric disorders, cardiovascular and cerebrovascular disease, cancer, endocrine disorders, treatment for drug and alcohol abuse, head trauma with loss of consciousness for more than five minutes, and alcohol consumption in excess of three drinks per day. All participants were strongly right-handed with scores over 75% on the Edinburgh Handedness Questionnaire (Oldfield, 1971). All participants completed a questionnaire to rule out current depression (CES-D; Radloff, 1977; cut-off = 15). An experimenter administered the Mini Mental Status Examination (MMSE; Folstein et al., 1975; cut-off = 26) to screen for cognitive impairment.

Participants carrying a diagnosis of essential hypertension and taking anti-hypertensive medications were included. In addition to diagnosis, they reported the number of years that they had been taking antihypertensive medication. Every participant's blood pressure was measured by a trained technician at least three times on different days, both at baseline and follow-up. Assessments used an auscultatory method to measure blood pressure with diastole phase V for identification of diastolic pressure (Pickering et al., 2005). The values were averaged across measurements to obtain the mean systolic and diastolic pressure reported in Table 1.

From the 104 participants scanned on two occasions, eight were subsequently excluded from analysis because of incidental findings, equipment malfunction, a drop in MMSE below 26, elevated CES-D scores, and newly diagnosed diabetes found at follow up. The sample analyzed here consisted of 96 participants including 66 women and 30 men (age at baseline: 19 to 78 years). Descriptive demographic statistics and comparisons by sex are listed in Table 1. Three participants in the study had baseline MMSE scores of 26 including a 46-year-old woman, a 66-year-old woman, and a 49-year-old man, all of whom improved by one or more points at follow up testing, and all of whom were normotensive.

2.2. Measures of vascular risk and metabolic risk indicators

After a 12-hr overnight fast, the participants underwent venipuncture and provided 20 cc of blood, which was analyzed for glucose, high- and low-density lipoprotein (HDL, LDL), and triglyceride levels at the Detroit Medical Center laboratory. Whole blood glucose levels were assessed by the standard enzymatic oxidase method, and the lipid panel by the direct cholesterol oxidase/cholesterol esterase method. Following blood collection, trained technicians measured the participant's clothed waist and hip circumference with a cloth tape measure.

Due to sample handling and processing errors, fasting blood glucose values were not determined for five participants (2f/3m) at baseline and six (4f/2m) at follow up. One male lacked baseline cholesterol data; follow up cholesterol values were unavailable for five participants (2f/3m). We coded these data as missing values and considered them missing at random.

2.3. MRI Imaging

DTI images were acquired as part of a longer protocol, using a 4T MRI scanner (Bruker Biospin, Ettlingen, Germany) equipped with an 8-channel head coil. The parameters of the

2-dimensional echo-planar diffusion-weighted sequence were as follows: repetition time = 4900 ms; echo time = 79 ms; 41 slices; slice thickness = 3 mm; distance factor = 0; field of view = 256 mm; matrix = 128 × 128; voxel size = 2.0 × 2.0 × 3.0 mm^3; generalized autocalibrating partially parallel acquisition acceleration factor = 2; and number of excitations = 10. Diffusion-weighted data were collected in six orthogonal gradient directions using diffusion weighting of 800 s/mm^2; an additional T2-weighted image was collected without diffusion weighting (b0 = 0 s/mm^2).

2.4. DTI Processing

DTI processing was performed using a custom pipeline, implemented in the FMRIB Software Library (FSL; Jenkinson et al., 2012) v5.0.2 (Analysis Group, FMRIB, Oxford, UK). The pipeline was designed to maintain the original signal characteristics of data from both measurement occasions and minimize undue interpolation due to spatial transformation. A complete description of all processing steps is provided in Supplemental Information (SI). Briefly, this was achieved by using the tract-based spatial statistics (TBSS; Smith et al., 2006) processing pipeline for skeletonization of fractional anisotropy (FA) data following standard tensor fitting. TBSS processing used the FMRIB58_FA standard space image as the target for non-linear registration and a threshold of 0.3 for the final processing step. The resultant mean WM skeleton mask and the skeletonized regions of interest (ROIs) formed by the intersection of the WM skeleton mask with the International Consortium of Brain Mapping (ICBM)-DTI-81 WM atlas labels (Mori et al., 2005) at 1 mm, and the Johns Hopkins University (JHU)-WM tractography atlas (Wakana et al., 2007) were subsequently nonlinearly deprojected to native space (Foley et al., 2014). Prior to sampling, we sought to exclude cerebrospinal fluid (CSF) and areas of WMH from native space data by combining previous approaches for excluding CSF and accounting for the influence of WMH from DTI data (Davis et al, 2012; Sasson et al., 2010). The native b0 images were segmented into six classes, based on voxel intensity (SI Figure 1). Images corresponding to WM were summed and binarized to create a WM mask excluding CSF, areas of WMH, or image noise. DTI data used in analyses were sampled from native space data, masked for WMH and CSF, in 13 WM atlas-derived ROIs: corpus callosum (CC) genu, CC splenium, CC body, dorsal cingulum bundle (CBd), ventral cingulum bundle (CBv), superior longitudinal fasciculus (SLF), and two divisions of the internal capsule, the anterior limb (ALIC), and posterior limb (PLIC), inferior longitudinal fasciculus (ILF), inferior frontal-occipital fasciculus (IFOF), forceps major and forceps minor, and uncinate fasciculus (UF).

2.5. Data Conditioning & Analysis

All data were standardized to z-scores for analysis. Furthermore, in order to use standardized scores to calculate latent change scores, DTI data from the second occasion of measurement were standardized to the first measurement occasion. See SI for information on cases excluded from analysis due to inadequate signal.

The present study employed a structural equation modeling (SEM) framework to assess two-year change in DTI indices while controlling for individual differences in age, vascular risk, and inter-scan interval length. We first fit a series of univariate, two-occasion LCSMs (McArdle and Nesselroade, 1994; Figure 1A) for each of the three DTI indices. Although

brain volumetric measures appear stable over time in such models (Raz et al., 2005, 2008), only one other study has used this method for evaluating change in DTI indices (Lövdén et al., 2014). This analytic method is considered superior to standard linear modeling approaches for evaluating change for several reasons. First, the LCSM approach permits estimation of change on the level of a latent factor. By using such an SEM-based method, LCSM quantifies both mean latent change and variance or individual differences in change separately from their respective error variances. In contrast, traditional linear modeling approaches such as paired t-tests or repeated measures GLMs or ANOVAs possess the same shortcomings arising from the poor or uncertain reliability of raw difference scores. Moreover, traditional analytic methods assume but cannot quantify that variance in change is significant and that such variance may be explained by other variables.

We conducted the LCSM analyses in Mplus 7 (Muthén and Muthén, 2012) software using maximum likelihood (ML) estimation and treating missing data as missing completely at random (MCAR). We fit separate univariate LCSMs for each of the 13 ROIs sampled from the left and right hemispheres. The latent modeling approach assumes unobserved latent factors at baseline and follow-up. As in previous imaging studies using this analytic framework, mean left and right hemisphere values served as dual indicators for the latent factors at each occasion (Lövdén et al., 2014; Raz et al., 2005, 2008, 2010). Thus, the latent factor for each measurement occasion reflected combined variance from the two hemispheres (Fig. 1A). Additional information on the LCSM approach in modeling two-occasion change in brain structure is available elsewhere (Lövdén et al., 2014; Raz et al., 2005, 2008, 2010) and in SI.

Using a step-up approach (Raudenbush & Bryk, 2002), we initially fit LCSMs to the data without additional covariates. Such a method permits fine adjustment of LCSM specifications for each index and ROI to test for a significant mean difference between factors representing each measurement occasion or significant variance therein. The primary statistical concern for the LCSM procedure is the establishment of metric invariance, or the assumption that the relationship between observed and latent factors is invariant across measurements. A more detailed discussion of metric invariance is provided in SI (Meredith, 1964).

We assessed model fit using several indices: the comparative fit index (CFI) and Tucker-Lewis Index (TLI) were used to compare model fit to that of a null model, and values of .95 were cutoffs for both. For chi-square (X^2) tests of model fit, a nonsignificant ($p > .05$), smaller X^2 value indicates acceptable fit in comparison to a null model. A related, more informative fit statistic, X^2 divided by degrees of freedom (Jöreskog and Sörbom, 1993) used a fairly conservative cut-off value of ≤ 2.0 (Mueller, 1996). Additional goodness-of-fit indices included root mean square error of approximation (RMSEA), standardized root mean square residual (SRMR), measures of model misspecification and explained variance, respectively. For both the RMSEA and SRMR, acceptable fit was indicated by values of .08 and below.

Next, a new series of LCSMs was performed as before, but with the addition of four covariates: baseline age (in months), sex, interval between scans (in months) and self-

reported years taking hypertension medications at follow up, all continuous measures standardized to z-scores. The covariate models were only evaluated for those univariate models demonstrating significant variance in change. These LCSMs specified paths from all three covariates to the latent change score factor, and correlations between the Time 1 factor and both age and years on high blood pressure (HBP) medications, while constraining residualized correlations between the Time 1 factor and inter-scan interval to zero. We re-specified each model to exclude or constrain to zero those continuous covariate model parameters that produced non-significant ($p > .4$) parameter estimates close to zero. Similarly, nonsignificant dichotomous parameters were excluded from the final models.

Although inclusion of duration of antihypertensive treatment as a covariate in the univariate LCSMs was intended to address the influence of hypertension on change in WM, it is possible such an approach may not fully reflect the influence of hypertension or treatment in these models. Thus, following assessment of univariate models, we refit the univariate LCSMs without covariates, excluding participants who reported using antihypertensive medication at either wave of assessment. Next, this approach was repeated while omitting all participants who reported diagnosed hypertension or who reported taking cholesterol-reducing medications (e.g., statins or selective inhibitors of cholesterol absorption) at either measurement occasion, given the possible confounding influence of such medications on WM decline.

Last, we examined the influence of a latent physiological factor representing metabolic syndrome (Met) on individual differences in WM change. First, we used confirmatory factor analysis (CFA) to establish a latent factor for Met (Figure 1B) and tested its metric invariance across measurement occasions via univariate LCSM. Based on the results of the CFA and univariate LCSM for Met risk, we then specified multivariate LCSMs for each WM ROI and DTI index showing significant variance in change to test whether baseline values or change in Met predicted change in DTI measures (Figure 1C). Finally, we repeated the multivariate LCSMs evaluating metabolic syndrome as a predictor of change in WM value after removing participants reporting diagnosed hypertension or use of anti-hyperlipidemic medications.

Due to the large number of models fit to the DTI data, we applied a correction for false discovery rate (FDR; Benjamini and Hochberg, 1995; Pike, 2011) to significance values for latent change factors and variance of mean change from univariate LCSMs. We also calculated Cohen's *d* effect size statistic for mean change estimates by dividing the mean latent change parameter estimate by the standard deviation of the baseline DTI factor.

3. Results

3.1 Univariate LCSMs without Covariates

We fitted 39 univariate LCSMs to the data for the three DTI indices and all 13 ROIs containing bilateral indicators. All models, specified to converge free of errors, while maintaining factorial invariance, fit well according to multiple goodness-of-fit indices: X^2 range = 0.08 to 12.85, all $p \geq .12$, CFI ≥ 0.95, TLI ≥ 0.96, RMSEA values ≤ 0.79. However, in two instances (for ALIC RD and SLF RD), acceptable model fit was attained only by

freely estimating one indicator intercept. Spaghetti plots detailing patterns of change in DTI over time are shown in Figures 2-4.

Results from the univariate LCSMs are presented in Table 2. As depicted in Figure 5A, the models revealed significant two-year reductions in AD in all association fiber ROIs (i.e., CBd, CBv, IFOF, ILF, SLF, UF; Figure 2), and in both of the modeled projection fiber regions (ALIC and PLIC; Figure 4). In contrast, rostral commissural regions CC genu and forceps minor evidenced significant mean increases in AD (Figure 3). The univariate LCSMs on RD showed a markedly different pattern: whereas RD in CBv and PLIC showed significant mean declines, it increased in IFOF. Furthermore, the models revealed significant increases in RD in both rostral and caudal commissural regions (i.e., CC genu and splenium, forceps major, and forceps minor), accompanied by significant RD decreases in CC body. FA showed a significant mean decrease in IFOF, CC genu, and both forceps minor and forceps major, whereas increased FA was observed only in PLIC and CC body.

Significant variance in change was evident in multiple regions (Figure 5B). All three DTI indices exhibited individual differences in change in CC body, forceps minor, and SLF. Variance in RD and FA change was significant within CBd, IFOF, UF, and ALIC. Significant variance in change in PLIC was observed only for RD. Across indices, no significant individual differences in change were observed for CBv, CC genu or splenium, forceps major, or ILF.

3.2 DTI Measurement Stability

To assess the stability of the DTI measures, we calculated zero-order correlations (Pearson's *r*) between Time 1 and Time 2 observed mean values for the three DTI indices for each of the 13 ROIs, separately for left and right hemispheres (SI Table S1). In addition, we extracted the latent change factor score from each of the univariate LCSMs without covariates and calculated correlations between baseline and follow up for each index and ROI. As evident from Table S1, despite substantial variations by region and index, the use of dual indicators to form latent factors resulted in dramatic improvements in test-retest stability across all models.

3.3. Predictors of Individual Differences in Change: Univariate LCSMs – Covariate Models

The addition of the covariates (age, years on anti-hypertensive medications, and interval between scans) to the LCSMs allowed us to gauge the influence of these variables on change. Furthermore, this permitted comparison of mean change with cross-sectional age differences in the DTI indices. Following final specification, all models converged free of errors, and without violating factorial invariance assumptions. The covariate models revealed significant effects following FDR correction. In ALIC, advanced age was associated with greater mean decrease in AD (est./S.E. = 2.42, p = .016, corrected). More years of diagnosed hypertension were linked with greater FA increases in CC body (est./S.E. = 2.12, p = .026, corrected).

We observed significant sex differences. Female participants had higher baseline AD in forceps minor (est./S.E. = 2.55, p = .011, corrected) and lower RD in CC body (est./S.E. =

2.31, p = .021, corrected). A significant effect of sex on FA change in forceps minor (est./S.E. = 2.31, p = .024, corrected) was probed with univariate LCSMs grouped by sex. Although both men and women exhibited significant variance in FA change (p < .001), only women showed significant mean FA decline in forceps minor (est./S.E. = −5.36, p < .001), with no significant change observed among men (est./S.E. = −0.50, p = .618). Moreover, more years of medicated hypertension was significantly related to lower baseline forceps minor FA only for women (est./SE= −3.15, p = 0.002) but not men (p = 0.899). A similar effect of sex on FA change was observed in SLF (est./S.E. = 2.80, p = .005). Sex-grouped univariate LCSMs without covariates showed that only women exhibited significant variance in change (est./SE = 2.76, p = 0.006) and significant mean change (est./SE = −2.69, p = 0.007), but not men (p > .099 for both). Longer treatment for hypertension was significantly related to increased SLF FA decline for women (est./SE= −2.05, p = 0.041), but not men (est./SE= 0.71, p = 0.478).

In addition to testing covariate effects via direct paths from covariates to the change factor, univariate LCSMs with covariates examined bidirectional associations, or auto-correlated residuals between baseline measures of age and DTI indices. These analyses showed that greater age was associated with higher RD and lower FA in all ROIs, and with lower AD in forceps minor and forceps major. Longer time since diagnosis of hypertension was associated with higher RD and with lower FA in IFOF and CC body. A comparison of baseline age-DTI associations and mean change, by DTI index and ROI is shown in Table 3.

3.4. Subsidiary Analyses – Normotensive Subsample

To clarify the influence of medically treated hypertension, we evaluated the univariate LCSMs after excluding participants who reported taking antihypertensive medications (n = 20). Following FDR correction, exclusion of hypertensive participants rendered the mean change in AD of UF and RD of CBv, nonsignificant (Table 4). Univariate models in a sample restricted to normotensive participants showed significant two-year decline of FA in CC splenium, a region that evidenced no significant mean change in the whole sample. In addition, variance in change was no longer significant in RD models of ALIC, IFOF, SLF, and UF, and in FA models of SLF and UF. However, even after accounting for the influences of medicated hypertension, we still observed significant individual differences in change in several regions, including all three indices in forceps minor and CC body, FA and RD in both CBd and PLIC, FA in IFOF, and AD in SLF.

Twelve of the 76 normotensive participants reported taking medication for reduction of blood cholesterol levels, and for two participants, the relevant medication status was unknown. In order to assess the possible influence of these medications (mainly statins) on WM change, we re-evaluated the models for the remaining 62 participants. After exclusion of participants taking anti-hyperlipidemic medications, the models no longer showed significant mean change in RD for CC splenium. Moreover, RD in IFOF, and FA in PLIC no longer showed significant individual differences in change. All other effects remained unchanged.

3.5. Modeling Change with Metabolic Risk Factors Index as a Covariate

Excluding the data for those reporting use of antihypertensive medications, we first specified a CFA model using baseline Met indicators: log-transformed triglyceride level, HDL cholesterol level, systolic blood pressure, waist-to-hip ratio, and fasting blood glucose level.

Although initial model fit was acceptable, the results of subsequent steps to establish factorial invariance between the two measurement occasions necessitated omitting HDL from the model (see SI for a complete description of those analyses). The new LCSM of Met score without HDL was a good fit for the data ($X^2[31] = 21.90$, $p = .886$, CFI/TLI = 1.00/1.03, RMSEA = 0.00, SRMR = 0.06), but the estimated variance in the change score was no longer significant (estimate/S.E. = 1.79, $p = .074$).

Next, we created a series of multivariate LCSMs using the Met-including model in combination with each of the 12 DTI models (Figure 2C) that showed significant variance in change in the normotensive sub-sample. These included all three DTI indices for CC body and forceps minor, FA and RD models for CBd and PLIC, FA for IFOF, and AD for SLF. We used the Met LCSM rather than simply the baseline CFA, because having two occasions in the model demonstrating factorial invariance should provide a more stable factor than a single occasion. For each multivariate model, we specified direct paths from baseline age to the baseline Met factor and from the baseline Met factor to the DTI latent change score factor. In addition, we specified the model to test for indirect effects of age on DTI indices in order to test whether the effects of age on change in DTI measures were mediated by Met. Indirect effects were computed as the products of the constituent direct path parameter estimates (Cheung, 2009). Confidence intervals for significant indirect effects were constructed using bias-corrected bootstrap resampling with 5000 draws. Bias-corrected bootstrapped confidence intervals (CIs) for indirect effects provide superior measures of mediation (MacKinnon et al., 2002) in comparison to other common approaches (i.e., Baron and Kenny, 1986). We obtained very good fit in all models, although the model for FA in forceps minor had acceptable fit only if a path was specified between baseline measures of age and WM.

Four models contained significant direct paths from the baseline Met factor to change in DTI indices. In the models for CC body, higher baseline Met predicted increases in RD ($p < .00$) and reductions in FA ($p < .01$). In CBd models, higher Met score at baseline predicted greater increases in RD ($p = .01$) and reductions in FA ($p = .02$). Furthermore, there were significant indirect effects of Age → Met → change in CC body RD (estimate/S.E. = 2.79, $p < .01$, 95% CI = 0.06 to 0.26) and FA (estimate/S.E. = −2.81, $p < .01$, 95% CI = −0.36 to −0.11). There were also significant indirect effects of Age → Met → change in CBd RD (estimate/S.E. = 2.13, $p < .05$, 95% CI = 0.05 to 0.32) and FA (estimate/S.E. = −2.22, $p < .05$, 95% CI = −0.39 to −0.03). Thus, in models of FA and RD for CC body and CBd, the metabolic syndrome factor mediated the effects of age on two-year change: older participants with increased levels of the Met indicators showed greater change in these regions. However, R^2 statistics revealed that only for the CC body FA and RD models, did Met factor account for a significant proportion of variance in two-year change (for both, p

< .05). Re-evaluation of the mediation models after removal of anti-hyperlipidemic medication users revealed the same pattern of results and indirect effects.

4. Discussion

This study demonstrates reliable change over two years in all DTI indices of normally appearing cerebral WM in healthy adults covering a wide age range. The novel finding is that the rate of change varies significantly across multiple white matter regions and among individuals. This is in contrast to cross-sectional associations between age and WM measures that suggested largely uniform age-related WM deterioration across brain regions. Notably, these changes were observed in normally appearing WM, after excluding the potentially confounding effect of WMH, and were exacerbated by metabolic risk. Thus, our findings add to the growing body of evidence showing limited validity of cross-sectional estimations of change. Even when cross-sectional findings correctly identify mean trends, they cannot capture the temporal dynamics of normal WM and may misrepresent age-related change (Hofer et al., 2006). Moreover, cross-sectional methods are incapable of addressing the important issue of individual variability of brain aging trajectories or testing for mediation effects in studies of neurocognitive aging (Lindenberger et al., 2011; Maxwell & Cole, 2007).

Neurobiological underpinnings of the observed changes in WM are unclear. Advanced age is associated with increased occurrence of myelin sheath deformations (Bowley et al., 2010; Peters, 2002), fewer small-diameter myelinated fibers (Marner et al., 2003; Tang et al., 1997), expanded extra-axonal spaces, and loss of anterior commissural fibers, but not with axonal degeneration (Budde et al., 2009; Nielsen and Peters, 2000; see Beaulieu 2002, 2012 for reviews). Age-related WM differences such as increased axonal diameter and reduced packing density could result in increased diffusivity and reduced FA. Although myelin influences both FA and RD (Song et al., 2002; 2006; Sun et al., 2008), those indices are poor proxies for local myelin content (Beaulieu, 2012; De Santis et al., 2014; Kolind et al., 2008; Mädler et al., 2008). Axonal diameter, independent of myelination, appears the strongest anatomical correlate of AD (Beaulieu, 2012). Despite the challenges inherent in interpreting differential patterns of DTI indices in terms of underlying tissue characteristics (Wheeler-Kingshott & Cercignani, 2009), comparison of our findings with those from prior DTI and histology studies may be helpful in understanding different patterns of WM change.

4.1 Mean Change in Diffusion-Based Descriptors of WM Organization

One of the most notable findings in this study is significant reduction in AD in all examined association fiber ROIs and in both of the modeled projection fiber regions. In five regions, CBd, ILF, SLF, UF, and ALIC the decline in AD was not accompanied by change in other indices. In other words, WM microstructure of these tracts changed in such a way that reduced likelihood of diffusion in the principal direction of the tensor was unaccompanied by alterations in RD or anisotropy. The observed AD reduction may stem from increases in axon diameter, or myelin sheath deformation (i.e., myelin “ballooning’ or “splitting’) that produces additional barriers to parallel diffusion (see Peters, 2002, Beaulieu 2002, 2012 for reviews). These changes in healthy adult brains may be qualitatively different from

alterations observed in chronic WM pathology such as multiple sclerosis and amyotrophic lateral sclerosis (ALS), in which reductions in AD and FA appear to go hand in hand (Fox et al. 2011, Menke et al., 2012). However, in at least one region (IFOF) we found that reduction in AD was accompanied by increased RD and reduced FA, which is consistent with possible mean regional changes in myelin sheath integrity, axonal fiber packing density or fiber coherence.

Unlike ALIC, all three DTI-derived indices showed changes in PLIC, including declines in both diffusivity measures and increase in FA. The reasons for this discrepancy are unclear but they may stem from distinct developmental and structural characteristics of this part of the internal capsule (IC). Fibers in PLIC are myelinated earlier, show greater coherence, and tend to include more axons with large diameters than those in the anterior portions of the IC (Axer and Keyserlingk, 2000). In normal brains, FA in PLIC increases from infancy into adolescence and through young adulthood, and is positively correlated with motor skill learning and development (Madhavan et al., 2014; Qiu et al., 2008; Wang et al., 2013). This pattern is in stark contrast with findings from studies of the WM afflicted by neurodegenerative disease. Whereas we observed longitudinal mean increases in PLIC FA and reductions in AD, in patients suffering from ALS, AD in PLIC increases over the course of disease, and FA reduction in PLIC predicts more severe symptom progression. It is possible that in adults who are older and less healthy than the participants of our study, a degenerative pattern emerges in all regions of IC. However, in people who are in good health, PLIC may show extended development into late adulthood.

Two-year change in the commissural fibers was markedly different from that of the association fiber regions. Moreover, we noted an anterior to posterior gradient of change (Head et al., 2004). In contrast to almost uniform AD decline in all association and projection regions, longitudinal AD increased in rostral commissural fibers. Furthermore, these changes were accompanied by increases in RD and reductions in FA. Although the signal from voxels in the forceps minor ROI could plausibly be influenced by adjacent fiber populations with different properties or orientations (Malykhin et al., 2011), such influence is unlikely in the more limited CC genu ROIs. Increases in both diffusivity indices in conjunction with reduced FA could correspond to reductions in myelin content, expansion of extra-axonal space or increase in proportion of fibers with large axons. Moreover, we observe a similar pattern, but without change in AD in the CC splenium. CC body showed a markedly different pattern of change, with increases in FA and reductions in RD but no change in AD. Like CC body, posterior commissural regions (CC splenium and forceps major) also evidence no mean change in AD. However, more similar to anterior regions, CC splenium and forceps major show increases in RD, while decreased FA was only observed in the latter region. These differences in change may reflect differences in axonal size and morphology of the fiber population in these regions. Histological studies of CC in rodents have shown a preponderance of smaller-diameters axons in anterior and posterior regions, and increase in larger-diameter axons in the mid-body (Barazany et al., 2009). Thus, age-related reductions in the proportion of smaller-diameter axons may also account for some of these differences. In addition, it is plausible, though not at all demonstrable at this point, that white matter damage in the prefrontal regions precedes changes in the rest of the brain where age-related changes are delayed beyond the age range sampled in this study (Davis et

al., 2009; Head et al., 2004). Although such state of affairs would be consistent with heterochronicity hypothesis of WM aging, many more measurement occasions in a wider age range would be needed to test this proposition (Lindenberger et al., 2011).

4.2 Individual Differences in Change

Individual differences in brain aging stem from multiple factors, and only a few of them can be examined in a single sample without risking capitalization on chance. In this study, theoretically relevant covariates explained some variance in change, although the nature of such influence is not clear. Significant individual differences in two-year change were observed in multiple regions. In some (CC body, forceps minor and SLF) individual variability of change involved all three DTI indices, in others, the observed individual differences were restricted to one or two of the DTI-based indicators. Variance in RD and FA change was significant within CBd, IFOF, UF, and ALIC. Significant variance in change in PLIC was observed only for RD. Notably, no significant individual differences in change were observed for CBv, CC genu or splenium, forceps major, or ILF. This is in contrast to individual variations in change of parenchymal volume across almost all examined brain regions that we have observed in several samples (Raz et al., 2005; 2010; Persson et al., 2014).

Identifying sources of individual variability of WM changes is important for understanding successful aging. From our necessarily limited evaluation of sources of such variability, we observed that at least in one region, ALIC, age was positively associated with decrease in AD. To some extent, this finding is consistent with the hypothesis that hampered diffusion along the axons in that projection tract may result from cumulative damage over time (Beaulieu, 2002). Steeper AD declines within ALIC were not observed in PLIC, another region of major projection fiber tracts. Although the source of this discrepancy is unclear, organizational differences in the sampled regions may provide a clue to possible sources of discrepant findings. Whereas ALIC includes thalamo-cortical-striatal, cortico-pontine, and intra-striatal fibers that vary substantially in their orientation, PLIC fibers included in this ROI are more uniformly orientated and include greater numbers of larger-diameter axons (Axer and Keyserlingk, 2000). Thus, PLIC appears more likely to evidence diffusion-related stability over time.

Individual differences in vascular risk and in responses to intervention aimed at its alleviation constitute plausible sources of individual variability in change. Indeed, we observed that longer duration of self-reported treatment for hypertension was associated with lower baseline FA, and greater increases of FA over time in CC body. This finding suggests that although short-term intervention in hypertension yielded no significant improvement in macrostructural indices of brain aging, earlier diagnosis of vascular risk and timely intervention may prevent deterioration of the WM. To date, no longitudinal intervention studies of hypertension and microstructural changes in the WM are available, and the long-term benefits of anti-hypertensive medication regimen for brain health have not been established (Jennings et al., 2012). In addition, the present findings showed regionally specific sex differences in WM characteristics. Furthermore, duration of hypertension treatment was associated with lower baseline FA in forceps minor and with greater FA

decline in SLF only for women. Although it is possible that men may have shown significant change and variance therein in SLF models of FA with greater power, the null effects observed in other regions suggest this may be a more isolated phenomenon.

Individual variance in change is not restricted to older adults but was observed across a wide age range sampled in this study. In addition, we were able to identify potential sources of variability in change within a more selected group – persons who had no diagnosed hypertension. In this optimally healthy subsample, metabolic syndrome risk factor indicators showed significant association with change in WM microstructure. In the models for CC body and CBd, higher metabolic risk at baseline predicted increases in RD and reductions in FA – a pattern that may indicate demyelination (Beaulieu, 2002). This suggests that even a clinically unremarkable elevation in metabolic syndrome risk may predict deterioration of WM within a relatively narrow time window. Moreover, at least for these two regions, metabolic syndrome risk mediated the effects of age on two-year change: younger participants with increased levels of the metabolic risk indicators showed greater decline in these regions, whereas low levels of metabolic risk appeared protective in older adults. Although myelination may continue into older age (see Bartzokis, 2011 for a review), the negative effects of concomitant increases in vascular and metabolic risks may be linked with its ultimate decline (Ryu et al., 2014). Conversely, it is possible increased cardiovascular fitness may ameliorate such influence in older age (Tseng et al., 2013). Unfortunately, in the present study are did not have sufficient information about participants physical activity to address such a possibility.

Placing the present findings into a larger context of extant reports is important. Unfortunately, this aspect of interpreting our results is hindered by the fact that to date, only three studies of adults examined age-related changes in DTI-derived measures of white matter structure, over a similar period of about two years. Sullivan and colleagues (2010) used tractography and found no significant change in the CC in normal adults. The only study to assess regionally specific two-year change in a normal population of middle-aged and older adults (Barrick et al., 2010) used TBSS and voxel-wise paired t-test to evaluate differences in DTI indices between two measurement occasions. Importantly, neither study addressed the issue of individual differences in change. The latter is an important feature of our study. The study by Barrick et al. (2010) employed difference images and a permutation-based voxel-wise analysis, which necessitates perfect registration between occasions. In contrast, the methods employed in our study avoided that limitation as we performed LCSM analyses on mean values sampled from skeletonized ROIs deprojected to native spaces images, masked to exclude CSF and WMH. Furthermore, in light of suboptimal test-retest reliability of DTI measures (Landman et al., 2007; Madhyastha et al., 2014), it is possible that short-term voxel-wise comparison of difference images may reflect variation in measurement error more than meaningful changes in the signal of interest. The DTI sequence employed in the current study used 10 averages, which should mitigate such concerns. Moreover, the LCSM analytic framework used in the present study enabled analysis of change and quantification of variance therein at the level of a latent factor from which error variance has been removed.

A recent study of two-year change in relatively healthy octogenarians used methods similar to those employed here for ROI-based DTI sampling and statistical analysis (Lövdén et al., 2014). Although both studies found two-year FA reductions in CC genu, forceps major, forceps minor, and IFOF, only the study of very old adults showed significant mean longitudinal FA declines in SLF. Moreover, whereas that study reported significant individual differences in change across ROIs, significant variance in FA change in present study was limited to forceps minor, IFOF, and SLF, but not CC genu or forceps major. Comparison with the findings of Lövdén et al. (2014) is hampered by several substantive differences between the studies: exclusive use of mean diffusivity versus modeling AD and RD separately in this study, use of only six ROIs, confounding WMH with the normal appearing WM, and an almost complete lack of an overlap between sample age ranges.

Although our findings of AD increases in anterior WM are consistent with prior reports, an observation of decreasing mean AD across association and projection fibers is in contrast to the reported AD increases in PLIC and CBd in one previous study (Barrick et al., 2010). In our sample, increases in FA were noted in PLIC and CC body. This is in contrast to the widespread drop in FA (Barrick et al., 2010) and lack of CC change (Sullivan et al., 2010) found in other studies. In the former, these changes were also accompanied by longitudinal reductions in both diffusivity indices. Thus, deterioration of anterior white matter organization appears the only common finding in this limited sample of studies available to date. Unlike multiple discrepancies between cross-sectional and longitudinal findings, this conclusion is in accord with observation of age-related differences reported in cross-sectional studies (e.g., Head et al., 2004). Comparison of changes in anterior WM regions, particularly commissural and projection fibers and of age-related differences in the patterns of change across DTI indices represents an important objective for the study of brain and cognitive aging. Similarly, it is possible that comparison of changes in all DTI indices between CC body, genu and forceps minor may reveal anterior-posterior differences in trajectories of aging over longer periods of observation and grater number of measurement occasions than available in the current study.

As shown in Table 3, which compares correlations between age and DTI indices at baseline with two-year latent change, cross-sectional age differences do not reflect shorter-term dynamics of WM change. At any given moment, the state of WM microstructure reflects a dynamic equilibrium of many influences and there is no clear indication when and which of them exerts its effect on the shift in equilibrium and apparent decline. The discrepancies between cross-sectional age associations and actual patterns of change observed in the present study underscore an important issue in the study of aging: cross-sectional data can neither accurately model intra-individual change, nor can they inform about mediators of age on other systems (Hofer et al., 2001, 2006; Lindenberger et al., 2011). Although older age is clearly associated with WM deterioration, understanding the short- and long-term intra-individual temporal dynamics of WM microstructure remains an important aim for future investigation.

Importantly, the effects of participant selection in lifespan studies of healthy aging cannot be ignored. As shown in Figure 6, in our sample, the younger adults with subclinically elevated metabolic risk exhibited the greatest two-year decline in WM health in CC body and dorsal

cingulum, whereas the older adults with the lowest levels of metabolic risk showed the greatest improvements or stability in WM health. These findings suggest that the health conditions for which older participants were screened may be present in milder form in some younger adult participants, and that such selection for optimal health using the same criteria for all ages may obscure the effects of age. Moreover, this pattern is consistent with the possibility that physiological and neurobiological mechanisms driving WM change may vary with age. In younger and older adults, the same observed change in DTI-derived WM indices may represent different neurobiological underpinnings. Studies of age-related changes in other indices of WM integrity (e.g., Perrin et al., 2008; Paus, 2010), suggest that this may be the case.

4.3 Study Limitations and Future directions

Several factors may limit the generalizability of the present findings. By many accounts, tractography could provide more anatomically specific and less noisy DTI measures than our ROI approach. Despite the care that went into DTI processing, the use of an atlas-based system for anatomical designation is not as specific as tractography. Although ROIs did not overlap, neighboring regions such as ILF and IFOF, despite containing different variance, may not be as anatomically valid as streamlines. Unfortunately, as in many archival and longitudinal studies, we were bound by the initial choice of acquisition parameters and thus limited to six encoding gradient directions, making tractography unadvisable (Mukherjee et al., 2008).

Although others have employed similar approaches for ROI demarcation on skeletonized WM data (Foley et al., 2014), the outcome of TBSS skeletonization may be not highly reliable (Madhysatha et al., 2014; but see Jovicich et al., 2014). At the time of this writing, the degree to which the accuracy and reliability of TBSS skeletonization depends on other method variables, such as DTI acquisition parameters, or sample health or age has not been evaluated. Thus, important directions for future methodological investigations include comparing WM change when sampled from skeletonized and non-skeletonized WM. One concern is the WM skeleton may not have good correspondence with underlying WM structures identified in probabilistic atlases (Edden and Jones, 2011), particularly in areas such as the frontal lobes containing multiple fiber orientations (Bach et al., 2014; Malykhin et al., 2011). Although it may be exacerbated in pathological populations (Bach et al., 2014) or in aging, this limitation may be mitigated in the present study by applying strict exclusionary criteria in participant selection and by excluding WMH. Thus, the brains with significant neurodegenerative changes would be very unlikely to appear in this sample. Importantly, in our study, the use of latent variables rather than raw measures resulted in significantly improved stability of the estimates over time. Furthermore, although the MMSE is not a useful tool for diagnosis of cognitive impairment, especially in high-functioning individuals, it is a sensitive screening instrument (Kukull et al., 1994; Mitchell, 2009). Of eight participants with baseline MMSE scores below 28, one (MMSE=27) remained stable and seven improved by 1-3 points. Thus, although it is possible that in persons with the high level of education high MMSE scores could potentially mask nascent decline, the likelihood of such misclassification in this sample is very low.

In addition, although other software packages may provide superior registration, the re-fitting of tensors in the halfway registered space between the two occasions should at least ensure superior correspondence within subjects for WM skeletonization accuracy. Moreover, although CC and cingulum may not be easily separated following TBSS skeletonization (Bach et al., 2014), our deprojection of skeletonized ROIs to native space permitted inspection of all ROIs to establish specificity of correspondence on a case-by-case basis. Similarly, the contributions of image noise to false-positive tract center identification may be mitigated through exclusion of CSF and WMH. Furthermore, accurate interpretation of different combinations of FA, RD, and AD requires better understanding of other key influences on diffusion within a voxel, such as the presence of crossing fibers (Vos et al., 2012; Wheeler-Kingshott and Cercignani, 2009). Thus, controlling for such influences (Douaud et al., 2011) may bolster inferential speculation about spatial patterns of RD and AD, and correspondence with underlying cellular or pathological processes associated with aging.

Our analytic approach was an important advancement in evaluating individual differences in brain aging. However, because LCSM models required at least two indicators per latent factor, we were unable to model change of non-lateralized structures such as the fornix, which is considered a problematic region under any circumstances (Bach et al., 2014). Future studies employing more current, optimized imaging standards might be able to better delineate such structures for more reliable longitudinal comparison. Similarly, our reliance on mean values across atlas-based ROIs precluded greater localization of change.

4.5 Conclusions

Within a relatively narrow time window, we found widespread declines in AD in association and projection fibers, but observed AD increases in anterior commissural fibers. In contrast, RD increased in nearly all commissural regions, and caudal projection fibers also showed a marked increase. Furthermore, in healthy adults who were free of major clinically recognized vascular and metabolic risk factors, subclinical elevation in metabolic risk indicators mediated the effects of age on FA reductions and RD increases in selected regions. Notably, we observed little correspondence between direction of change inferred from cross-sectional age-related differences and actual change. Our findings underscore the importance of longitudinal studies evaluating individual differences in change, and the search for influential factors that may explain individual variability in the trajectories of healthy brain aging.

Supplementary Material

Refer to Web version on PubMed Central for supplementary material.

Acknowledgments

This work was based on the Ph.D. dissertation by ARB, and was supported in part by a grant from the National Institute on Aging R37-AG011230 to NR.

This study was supported in part by a grant from the National Institutes of Health R37-AG-11230 to NR.

References

Axer H, Keyserlingk DG. Mapping of fiber orientation in human internal capsule by means of polarized light and confocal scanning laser microscopy. J Neurosci Methods. 2000; 94(2):165–175. [PubMed: 10661836]

Bach M, Laun FB, Leemans A, Tax CM, Biessels GJ, Stieltjes B, et al. Methodological considerations on tract-based spatial statistics (TBSS). Neuroimage. 2014; 100:358–69. [PubMed: 24945661]

Barazany D, Basser PJ, Assaf Y. In vivo measurement of axon diameter distribution in the corpus callosum of rat brain. Brain. 2009; 132:1210–20. [PubMed: 19403788]

Baron RM, Kenny DA. The moderator-mediator variable distinction in social psychological research: Conceptual, strategic, and statistical considerations. J Pers Soc Psychol. 1986; 51(6):1173–1182. [PubMed: 3806354]

Barrick TR, Charlton RA, Clark CA, Markus HS. White matter structural decline in normal ageing: A prospective longitudinal study using tract-based spatial statistics. Neuroimage. 2010; 51(2):565–577. [PubMed: 20178850]

Bartzokis G. Alzheimer's disease as homeostatic responses to age-related myelin breakdown. Neurobiol Aging. 2011; 32(8):1341–71. [PubMed: 19775776]

Beaulieu C, Allen PS. Determinants of anisotropic water diffusion in nerves. Magn Reson Med. 1994; 31:394–400. [PubMed: 8208115]

Beaulieu C. The basis of anisotropic water diffusion in the nervous system - a technical review. NMR Biomed. 2002; 15(7-8):435–55. [PubMed: 12489094]

Beaulieu, C. The biological basis of diffusion anisotropy. In: Johansen-Berg, H.; Behrens, TE., editors. Diffusion MRI: From quantitative measurement to *In vivo* neuroanatomy. Academic Press; 2012. p. 106-26.

Benjamini Y, Hochberg Y. Controlling the false discovery rate: A practical and powerful approach to multiple testing. Journal of the Royal Statistical Society Series B (Methodological). 1995; 57:289–300.

Bolzenius JD, Laidlaw DH, Cabeen RP, Conturo TE, McMichael AR, Lane EM, Heaps JM, Salminen LE, Baker LM, Gunstad J, Paul RH. Impact of body mass index on neuronal fiber bundle lengths among healthy older adults. Brain Imaging Behav. 2013; 7(3):300–306. doi: 10.1007/s11682-013-9230-7. [PubMed: 23564371]

Bowley MP, Cabral H, Rosene DL, Peters A. Age changes in myelinated nerve fibers of the cingulate bundle and corpus callosum in the rhesus monkey. The Journal of Comparative Neurology. 2010; 518(15):3046–3064. [PubMed: 20533359]

Budde MD, Xie M, Cross AH, Song SK. Axial diffusivity is the primary correlate of axonal injury in the experimental autoimmune encephalomyelitis spinal cord: a quantitative pixelwise analysis. J Neurosci. 2009; 29(9):2805–13. [PubMed: 19261876]

Burgmans S, van Boxtel MP, Gronenschild EH, Vuurman EF, Hofman P, Uylings HB, et al. Multiple indicators of age-related differences in cerebral white matter and the modifying effects of hypertension. Neuroimage. 2010; 49(3):2083–2093. [PubMed: 19850136]

Charlton RA, Schiavone F, Barrick TR, Morris RG, Markus HS. Diffusion tensor imaging detects age related white matter change over a 2 year follow-up which is associated with working memory decline. J Neurol Neurosurg Psychiatry. 2010; 81(1):13–19. [PubMed: 19710050]

Cheung MW. Comparison of methods for constructing confidence intervals of standardized indirect effects. Behav Res Methods. 2009; 41(2):425–438. [PubMed: 19363183]

Davis SW, Dennis NA, Buchler NG, White LE, Madden DJ, Cabeza R. Assessing the effects of age on long white matter tracts using diffusion tensor tractography. Neuroimage. 2009; 46(2):530–541. [PubMed: 19385018]

Davis SW, Kragel JE, Madden DJ, Cabeza R. The architecture of cross-hemispheric communication in the aging brain: linking behavior to functional and structural connectivity. Cereb Cortex. 2012; 22:232–42. [PubMed: 21653286]

DeCarli C, Murphy D, Tranh M, Grady C, Haxby JV, Gillette J, Salerno JA, Gonzales-Aviles A, Horwitz B, Rapoport SI, Shapiro MB. The effect of white matter hyperintensity volume on brain

structure, cognitive performance, and cerebral metabolism of glucose in 51 healthy adults. Neurology. 1995; 45:2077–2084. [PubMed: 7501162]

De Santis S, Drakesmith M, Bells S, Assaf Y, Jones DK. Why diffusion tensor MRI does well only some of the time: variance and covariance of white matter tissue microstructure attributes in the living human brain. Neuroimage. 2014; 89:35–44. [PubMed: 24342225]

Debette S, Seshadri S, Beiser A, Au R, Himali J, Palumbo C, et al. Midlife vascular risk factor exposure accelerates structural brain aging and cognitive decline. Neurology. 2011; 77(5):461–468. [PubMed: 21810696]

Douaud G, Jbabdi S, Behrens TE, Menke RA, Gass A, Monsch AU, et al. DTI measures in crossing-fibre areas: increased diffusion anisotropy reveals early white matter alteration in MCI and mild Alzheimer's disease. Neuroimage. 2011; 55(3):880–890. [PubMed: 21182970]

Edden RA, Jones DK. Spatial and orientational heterogeneity in the statistical sensitivity of skeleton-based analyses of diffusion tensor MR imaging data. J Neurosci Methods. 2011; 201(1):213–9. [PubMed: 21835201]

Ervin RB. Prevalence of metabolic syndrome among adults 20 years of age and over, by sex, age, race and ethnicity, and body mass index: United States, 2003-2006. Natl. Health Stat. Rep. 2009; 13:1–7.

Foley JM, Salat DH, Stricker NH, Zink TA, Grande LJ, McGlinchey RE, et al. Interactive effects of apolipoprotein E4 and diabetes risk on later myelinating white matter regions in neurologically healthy older aged adults. Am J Alzheimers Dis Other Demen. 2014; 29(3):222–35. [PubMed: 24381137]

Folstein MF, Folstein SE, McHugh PR. "Mini-mental state". A practical method for grading the cognitive state of patients for the clinician. J Psychiatr Res. 1975; 12(3):189–198. [PubMed: 1202204]

Ford ES, Giles WH, Dietz WH. Prevalence of the metabolic syndrome among US adults. JAMA: The Journal of the American Medical Association. 2002; 287(3):356–359.

Fox RJ, Cronin T, Lin J, Wang X, Sakaie K, Ontaneda D, et al. Measuring myelin repair and axonal loss with diffusion tensor imaging. AJNR Am J Neuroradiol. 2011; 32(1):85–91. [PubMed: 20947644]

Gouw AA, Seewann A, Vrenken H, van der Flier WM, Rozemuller JM, Barkhof F, et al. Heterogeneity of white matter hyperintensities in Alzheimer's disease: post-mortem quantitative MRI and neuropathology. Brain. 2008; 131:3286–3298. Pt 12. [PubMed: 18927145]

Gunning-Dixon F, Raz N. The Cognitive Correlates of White Matter Abnormalities in Normal Aging: A Quantitative Review. Neuropsychology. 2000; 14(2):224–232. [PubMed: 10791862]

Hannesdottir K, Nitkunan A, Charlton RA, Barrick TR, MacGregor GA, Markus HS. Cognitive impairment and white matter damage in hypertension: a pilot study. Acta Neurol Scand. 2009; 119(4):261–268. [PubMed: 18798828]

Head D, Buckner RL, Shimony JS, Williams LE, Akbudak E, Conturo TE, et al. Differential vulnerability of anterior white matter in nondemented aging with minimal acceleration in dementia of the Alzheimer type: evidence from diffusion tensor imaging. Cereb Cortex. 2004; 14(4):410–423. [PubMed: 15028645]

Hofer S, Flaherty B, Hoffman L. Cross-sectional analysis of time-dependent data: mean-induced association in age-heterogeneous samples and an alternative method based on sequential narrow age-cohort samples. Multivariate Behavioral Research. 2006; 41(2):165–187.

Hofer SM, Sliwinski MJ. Understanding ageing. Gerontology. 2001; 47(6):341–352. [PubMed: 11721149]

Hunt A, Orrison W, Yeo R, Haaland K, Rhyne R, Garry P, et al. Clinical significance of MRI white matter lesions in the elderly. Neurology. 1989; 39(11):1470–1470. [PubMed: 2812324]

Jacobs HI, Leritz EC, Williams VJ, Van Boxtel MP, van der Elst W, Jolles J, Verhey FR, McGlinchey RE, Milberg WP, Salat DH. Association between white matter microstructure, executive functions, and processing speed in older adults: the impact of vascular health. Hum Brain Mapp. 2013; 34(1): 77–95. doi: 10.1002/hbm.21412. Epub 2011 Sep 23. [PubMed: 21954054]

Jenkinson M, Beckmann CF, Behrens TE, Woolrich MW, Smith SM. FSL. Neuroimage. 2012; 62:782–90. [PubMed: 21979382]

Jennings JR, Mendelson DN, Muldoon MF, Ryan CM, Gianaros PJ, Raz N, Aizenstein H, Alzheimer's Disease Neuroimaging Initiative. Regional grey matter shrinks in hypertensive individuals despite successful lowering of blood pressure. J Hum Hypertens. 2012; 26(5):295–305. [PubMed: 21490622]

Jöreskog, KG.; Sörbom, D. LISREL 8: Structural equation modeling with the SIMPLIS command language. Scientific Software; Lincolnwood, IL: 1993.

Jovicich J, Marizzoni M, Bosch B, Bartres-Faz D, Arnold J, Benninghoff J, et al. Multisite longitudinal reliability of tract-based spatial statistics in diffusion tensor imaging of healthy elderly subjects. Neuroimage. 2014; 101:390–403. [PubMed: 25026156]

Kemper, TL. Neuroanatomical and neuropathological changes during aging and dementia. In: Albert, ML.; Knoefel, JE., editors. Clinical neurology of aging. 2nd. Oxford University Press; 1994. p. 3-67.

Kennedy KM, Raz N. Pattern of normal age-related regional differences in white matter microstructure is modified by vascular risk. Brain Research. 2009; 1297:41–56. [PubMed: 19712671]

Kolind SH, Laule C, Vavasour IM, Li DKB, Traboulsee AL, Mädler B, et al. Complementary information from multi-exponential T2 relaxation and diffusion tensor imaging reveals differences between multiple sclerosis lesions. Neuroimage. 2008; 40(1):77–85. [PubMed: 18226549]

Kukull W, Larson E, Teri L, Bowen J, McCormick W, Pfanschmidt M. The Mini-Mental State Examination score and the clinical diagnosis of dementia. J Clin Epidemiol. 1994; 47(9):1061–1067. [PubMed: 7730909]

Landman BA, Farrell JA, Jones CK, Smith SA, Prince JL, Mori S. Effects of diffusion weighting schemes on the reproducibility of DTI-derived fractional anisotropy, mean diffusivity, and principal eigenvector measurements at 1.5T. Neuroimage. 2007; 36(4):1123–1138. [PubMed: 17532649]

Lindenberger U, von Oertzen T, Ghisletta P, Hertzog C. Cross-sectional age variance extraction: what's change got to do with it? Psychol Aging. 2011; 26(1):34–47. [PubMed: 21417539]

Lövdén M, Köhncke Y, Laukka EJ, Kalpouzos G, Salami A, Li T-Q, et al. Changes in perceptual speed and white matter microstructure in the corticospinal tract are associated in very old age. NeuroImage. Aug 17.2014 102P2:520–530. [PubMed: 25139001]

MacKinnon DP, Lockwood CM, Hoffman JM, West SG, Sheets V. A comparison of methods to test mediation and other intervening variable effects. Psychol Methods. 2002; 7:83–104. [PubMed: 11928892]

Madden DJ, Bennett IJ, Burzynska A, Potter GG, Chen NK, Song AW. Diffusion tensor imaging of cerebral white matter integrity in cognitive aging. Biochim Biophys Acta. 2012; 1822(3):386–400. [PubMed: 21871957]

Madden DJ, Bennett IJ, Song AW. Cerebral white matter integrity and cognitive aging: contributions from diffusion tensor imaging. Neuropsychol Rev. 2009; 19(4):415–435. [PubMed: 19705281]

Madhavan S, Campbell SK, Campise-Luther R, Gaebler-Spira D, Zawacki L, Clark A, et al. Correlation between fractional anisotropy and motor outcomes in one-year-old infants with periventricular brain injury. J Magn Reson Imaging. 2014; 39(4):949–57. [PubMed: 24136687]

Madhyastha T, Mérillat S, Hirsiger S, Bezzola L, Liem F, Grabowski T, et al. Longitudinal reliability of tract-based spatial statistics in diffusion tensor imaging. Hum Brain Mapp. 2014 n/a-n/a.

Mädler B, Drabycz SA, Kolind SH, Whittall KP, MacKay AL. Is diffusion anisotropy an accurate monitor of myelination? Correlation of multicomponent T2 relaxation and diffusion tensor anisotropy in human brain. Magn Reson Imaging. 2008; 26(7):874–888. [PubMed: 18524521]

Maillard P, Carmichael O, Harvey D, Fletcher E, Reed B, Mungas D, et al. FLAIR and diffusion MRI signals are independent predictors of white matter hyperintensities. AJNR Am J Neuroradiol. 2013; 34(1):54–61. [PubMed: 22700749]

Malykhin N, Vahidy S, Michielse S, Coupland N, Camicioli R, Seres P, et al. Structural organization of the prefrontal white matter pathways in the adult and aging brain measured by diffusion tensor imaging. Brain structure & function. 2011; 216(4):417–31. [PubMed: 21559982]

Marks BL, Katz LM, Styner M, Smith JK. Aerobic fitness and obesity: relationship to cerebral white matter integrity in the brain of active and sedentary older adults. Br J Sports Med. 2011; 45(15):1208–1215. [PubMed: 20558529]

Marner L, Nyengaard JR, Tang Y, Pakkenberg B. Marked loss of myelinated nerve fibers in the human brain with age. The Journal of comparative neurology. 2003; 462(2):144–152. [PubMed: 12794739]

Maxwell SE, Cole DA. Bias in cross-sectional analyses of longitudinal mediation. Psychol Methods. 2007; 12(1):23–44. [PubMed: 17402810]

McArdle JJ, Hamgami F, Jones K, Jolesz F, Kikinis R, Spiro A, et al. Structural modeling of dynamic changes in memory and brain structure using longitudinal data from the normative aging study. The Journals of Gerontology Series B: Psychological Sciences and Social Sciences. 2004; 59:P294–P304.

McArdle, JJ.; Nesselroade, JR. Structuring data to study development and change. In: Cohen, SH.; Reese, HW., editors. Life-Span Developmental Psychology: Methodological Innovations. Erlbaum; Hillsdale, NJ: 1994. p. 223-267.

Menke RA, Abraham I, Thiel CS, Filippini N, Knight S, Talbot K, et al. Fractional anisotropy in the posterior limb of the internal capsule and prognosis in amyotrophic lateral sclerosis. Arch Neurol. 2012; 69(11):1493–9. [PubMed: 22910997]

Meredith W. Notes on factorial invariance. Psychometrika. 1964; 29(2):177–85.

Miralbell J, Soriano JJ, Spulber G, Lopez-Cancio E, Arenillas JF, Bargallo N, et al. Structural brain changes and cognition in relation to markers of vascular dysfunction. Neurobiol Aging. 2012; 33(5):1003. e1009-e1017. [PubMed: 22014619]

Mitchell AJ. A meta-analysis of the accuracy of the mini-mental state examination in the detection of dementia and mild cognitive impairment. J Psychiatr Res. 2009; 43(4):411–431. [PubMed: 18579155]

Mueller, RO. Basic principles of structural equation modeling: An introduction to LISREL and EQS. Springer Verlag; New York: 1996.

Mukherjee P, Chung SW, Berman JI, Hess CP, Henry RG. Diffusion tensor MR imaging and fiber tractography: technical considerations. AJNR Am J Neuroradiol. 2008; 29(5):843–852. [PubMed: 18339719]

Muthén, L.; Muthén, B. Mplus User's Guide. 6th. Muthén & Muthén; Los Angeles: 2012.

Nielsen K, Peters A. The effects of aging on the frequency of nerve fibers in rhesus monkey striate cortex. Neurobiol Aging. 2000; 21(5):621–628. [PubMed: 11016530]

O'Sullivan M, Barrick TR, Morris RG, Clark CA, Markus HS. Damage within a network of white matter regions underlies executive dysfunction in CADASIL. Neurology. 2005; 65(10):1584–1590. [PubMed: 16301485]

Oldfield RC. The assessment and analysis of handedness: the Edinburgh inventory. Neuropsychologia. 1971; 9(1):97–113. [PubMed: 5146491]

Paus T. Growth of white matter in the adolescent brain: myelin or axon? Brain Cogn. 2010; 72(1):26–35. [PubMed: 19595493]

Persson N, Ghisletta P, Dahle CL, Bender AR, Yang Y, Yuan P, et al. Regional brain shrinkage over two years: Individual differences and effects of pro-inflammatory genetic polymorphisms. Neuroimage. 2014; 103C:334–348. [PubMed: 25264227]

Peters A. The effects of normal aging on myelin and nerve fibers: a review. J Neurocyt. 2002; 31:581–593.

Perrin JS, Hervé PY, Leonard G, Perron M, Pike GB, Pitiot A, Richer L, Veillette S, Pausova Z, Paus T. Growth of white matter in the adolescent brain: role of testosterone and androgen receptor. J Neurosci. 2008; 28(38):9519–9524. [PubMed: 18799683]

Pickering TG, Hall JE, Appel LJ, Falkner BE, Graves J, Hill MN, et al. Recommendations for blood pressure measurement in humans and experimental animals. Hypertension. 2005; 45(1):142–161. [PubMed: 15611362]

Pike N. Using false discovery rates for multiple comparisons in ecology and evolution. Methods Ecol Evol. 2011; 2(3):278–282.

Qiu D, Tan LH, Zhou K, Khong PL. Diffusion tensor imaging of normal white matter maturation from late childhood to young adulthood: voxel-wise evaluation of mean diffusivity, fractional anisotropy, radial and axial diffusivities, and correlation with reading development. Neuroimage. 2008; 41(2):223–232. [PubMed: 18395471]

Radloff LS. The CES-D scale: A self-report depression scale for research in the general population. Appl Psychol Meas. 1977; 1(3):385–401.

Raudenbush, SW.; Bryk, AS. Hierarchical linear models: Applications and data analysis methods. Sage; 2002.

Raz N, Ghisletta P, Rodrigue KM, Kennedy KM, Lindenberger U. Trajectories of brain aging in middle-aged and older adults: Regional and individual differences. Neuroimage. 2010; 51(2):501–511. [PubMed: 20298790]

Raz N, Kennedy KM. A systems approach to the aging brain: Neuroanatomic changes, their modifiers, and cognitive correlates. Imaging the aging brain. 2009:43–70.

Raz N, Lindenberger U, Ghisletta P, Rodrigue KM, Kennedy KM, Acker JD. Neuroanatomical correlates of fluid intelligence in healthy adults and persons with vascular risk factors. Cereb Cortex. 2008; 18(3):718–726. [PubMed: 17615248]

Raz N, Lindenberger U, Rodrigue KM, Kennedy KM, Head D, Williamson A, et al. Regional brain changes in aging healthy adults: General trends, individual differences and modifiers. Cereb Cortex. 2005; 15(11):1676–1689. [PubMed: 15703252]

Raz N, Rodrigue K. Differential aging of the brain: Patterns, cognitive correlates and modifiers. Neurosci Biobehav Rev. 2006; 30(6):730–748. [PubMed: 16919333]

Raz N, Yang Y, Dahle CL, Land S. Volume of white matter hyperintensities in healthy adults: contribution of age, vascular risk factors, and inflammation-related genetic variants. Biochim Biophys Acta. 2012; 1822(3):361–9. [PubMed: 21889590]

Ryu SY, Coutu J-P, Rosas HD, Salat DH. Effects of insulin resistance on white matter microstructure in middle-aged and older adults. Neurology. 2014; 82(21):1862–70. [PubMed: 24771537]

Sasson E, Doniger GM, Pasternak O, Assaf Y. Structural correlates of memory performance with diffusion tensor imaging. Neuroimage. 2010; 50(3):1231–42. [PubMed: 20045476]

Segura B, Jurado M, Freixenet N, Falcon C, Junque C, Arboix A. Microstructural white matter changes in metabolic syndrome. Neurology. 2009; 73(6):438. [PubMed: 19667318]

Schmidt R, Fazekas F, Kapeller P, Schmidt H, Hartung HP. MRI white matter hyper-intensities: Three year follow-up of the Austrian Stroke Prevention Study. Neurology. 1999; 53:132–139. [PubMed: 10408549]

Smith SM, Jenkinson M, Johansen-Berg H, Rueckert D, Nichols TE, Mackay CE, et al. Tract-based spatial statistics: voxelwise analysis of multi-subject diffusion data. Neuroimage. 2006; 31:1487–1505. [PubMed: 16624579]

Song SK, Sun SW, Ramsbottom MJ, Chang C, Russell J, Cross AH. Dysmyelination revealed through MRI as increased radial (but unchanged axial) diffusion of water. Neuroimage. 2002; 17(3):1429–1436. [PubMed: 12414282]

Stanek KM, Grieve SM, Brickman AM, Korgaonkar MS, Paul RH, Cohen RA, et al. Obesity Is Associated With Reduced White Matter Integrity in Otherwise Healthy Adults*. Obesity. 2010; 19(3):500–504. [PubMed: 21183934]

Sullivan EV, Rohlfing T, Pfefferbaum A. Longitudinal study of callosal microstructure in the normal adult aging brain using quantitative DTI fiber tracking. Dev Neuropsychol. 2010; 35(3):233–256. [PubMed: 20446131]

Sun SW, Liang HF, Cross AH, Song SK. Evolving Wallerian degeneration after transient retinal ischemia in mice characterized by diffusion tensor imaging. Neuroimage. 2008; 40(1):1–10. [PubMed: 18187343]

Tang Y, Nyengaard JR, Pakkenberg B, Gundersen HJ. Age-induced white matter changes in the human brain: a stereological investigation. Neurobiol Aging. 1997; 18(6):609–615. [PubMed: 9461058]

Teipel SJ, Meindl T, Wagner M, Stieltjes B, Reuter S, Hauenstein KH, et al. Longitudinal changes in fiber tract integrity in healthy aging and mild cognitive impairment: a DTI follow-up study. Journal of Alzheimer's disease : JAD. 2010; 22(2):507–522.

Tseng BY, Gundapuneedi T, Khan MA, Diaz-Arrastia R, Levine BD, Lu H, et al. White matter integrity in physically fit older adults. Neuroimage. 2013; 82:510–6. [PubMed: 23769914]

Vernooij MW, de Groot M, van der Lugt A, Ikram MA, Krestin GP, Hofman A, et al. White matter atrophy and lesion formation explain the loss of structural integrity of white matter in aging. Neuroimage. 2008; 43(3):470–477. [PubMed: 18755279]

Wang X, Casadio M, Weber KA 2nd, Mussa-Ivaldi FA, Parrish TB. White matter microstructure changes induced by motor skill learning utilizing a body machine interface. Neuroimage. 2013; 88C:32–40. [PubMed: 24220038]

Wheeler-Kingshott CAM, Cercignani M. About "axial" and "radial" diffusivities. Magn Reson Med. 2009; 61(5):1255–1260. [PubMed: 19253405]

Williams VJ, Leritz EC, Shepel J, McGlinchey RE, Milberg WP, Rudolph JL, et al. Interindividual variation in serum cholesterol is associated with regional white matter tissue integrity in older adults. Hum Brain Mapp. 2013; 34(8):1826–1841. [PubMed: 22438182]

Xu J, Li Y, Lin H, Sinha R, Potenza MN. Body mass index correlates negatively with white matter integrity in the fornix and corpus callosum: a diffusion tensor imaging study. Hum Brain Mapp. 2013; 34(5):1044–1052. [PubMed: 22139809]

Highlights

- Examined longitudinal white matter change in healthy aging with diffusion imaging
- Used latent statistical models to assess change and individual differences therein
- Axial diffusivity increased in anterior commissural regions, but declined elsewhere
- Metabolic risk mediated age effects on change in corpus callosum body and cingulum

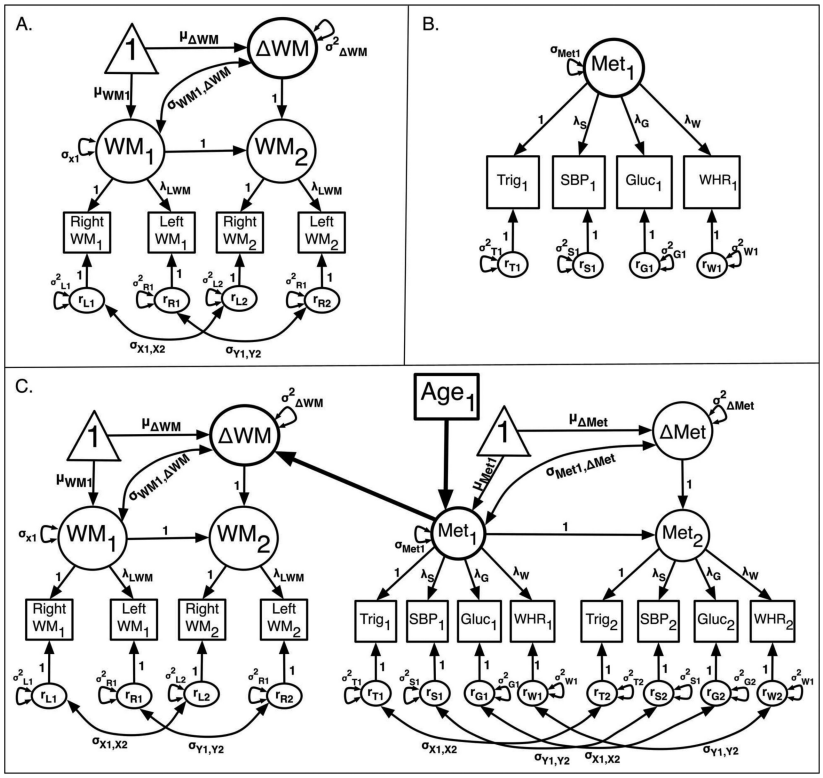

Figure 1.

Diagrams of measurement models used in the present study A. A generic univariate LCSM measurement model that was used in analyzing DTI data. The squares symbolize observed variables and the larger circles represent latent variables; WM1 and WM2 represent the latent white matter (WM) variable at Time 1 and Time 2, respectively. The triangle signifies means and intercepts for the latent change factor. The observed indicators Left WM and Right WM refer to left and right hemisphere measures from the same anatomical region. Auto-correlated residuals for observed variables are kept equivalent between occasions. The factor loading for the Left WM observed variables is fixed at 0, and an equivalency statement is imposed on the factor loadings for Y to maintain factorial invariance. For additional information on two-occasion latent change models, see McArdle and Nesselroade (1994). B. Final confirmatory factor analysis (CFA) structure used for modeling metabolic syndrome (Met). Indicators included baseline measures of triglycerides (Trig), systolic blood pressure (SBP), fasting blood glucose (Gluc) and waist-to-hip ratio (WHR). The factor loading for Trig was fixed to one for estimation, but all other factor loadings were freely estimated. C. Model evaluating baseline Met as a mediator of the effects of baseline age on change in WM.

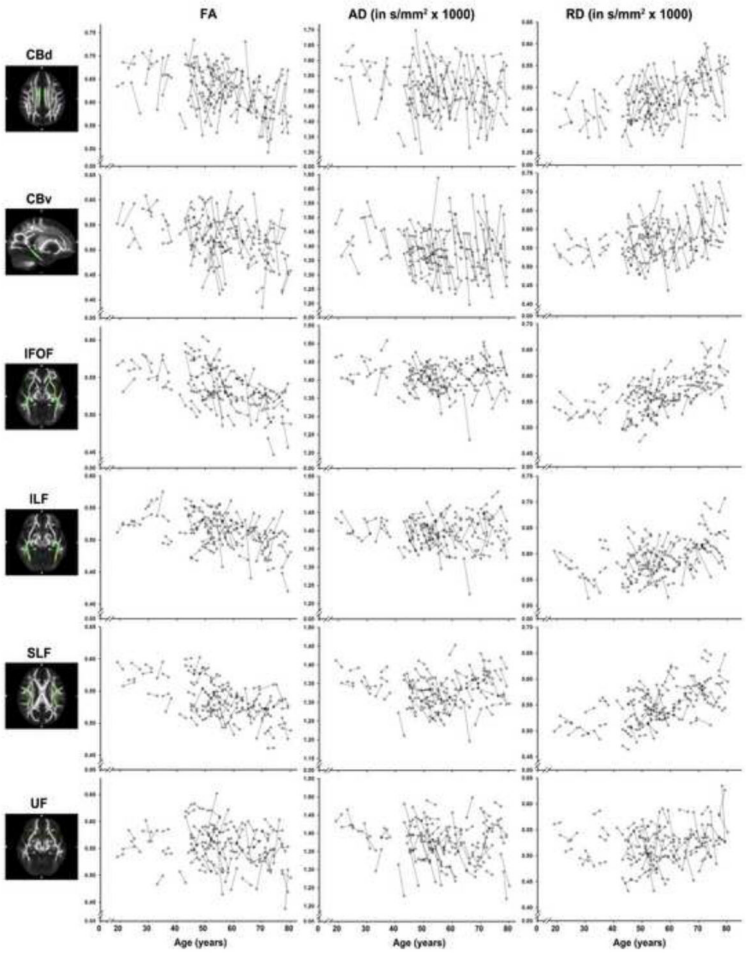

Figure 2.
Longitudinal change in FA (left column), AD (middle column) and RD (right column) for association tract ROIs as a function of baseline age.

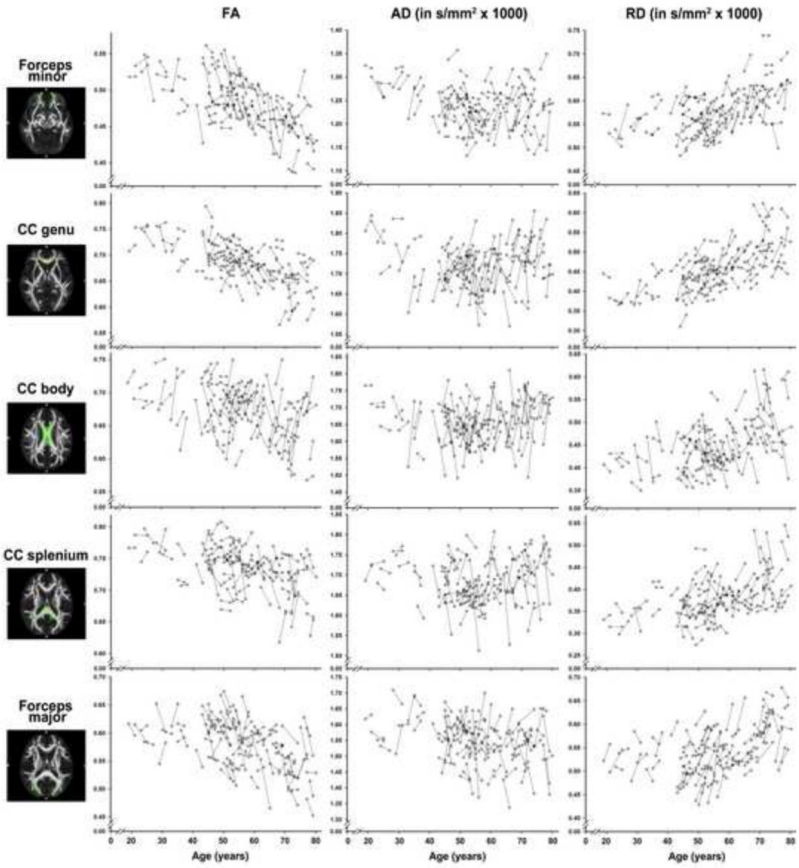

Figure 3.

Longitudinal change in FA (left column), AD (middle column) and RD (right column) for commissural tract ROIs as a function of baseline age.

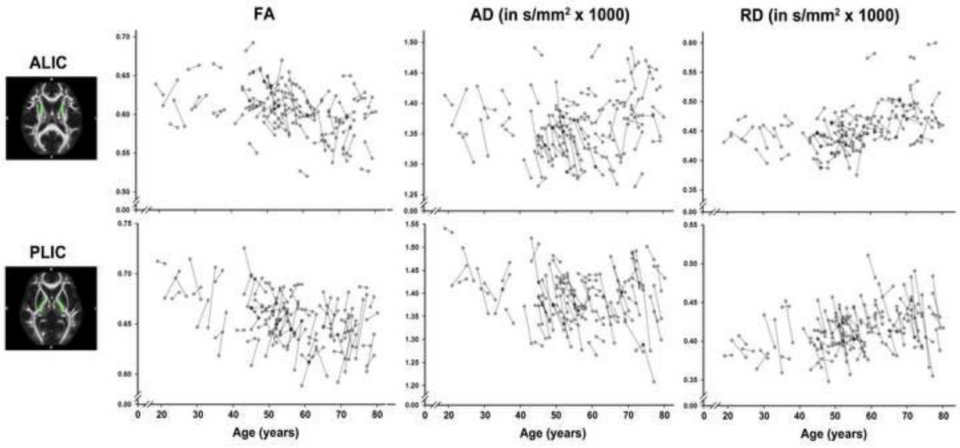

Figure 4.

Longitudinal change in FA (left column), AD (middle column) and RD (right column) for projection tract ROIs as a function of baseline age.

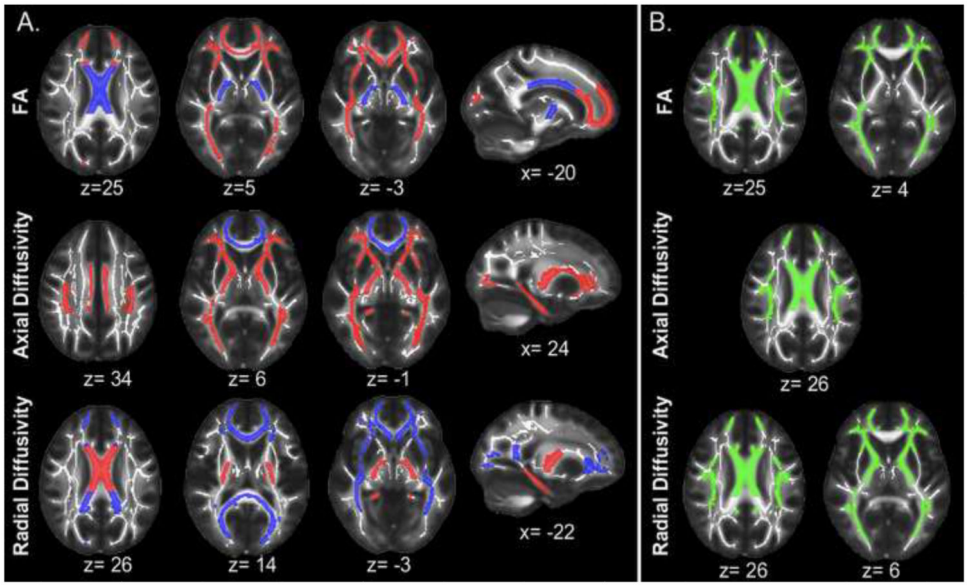

Figure 5.

A. Regions of interest (ROIs) showing significant two-year mean change in three DTI-derived indices. The mean FA skeleton mask (white) is superimposed over the FMRIB58 1 mm FA image. Skeletonized atlas regions were dilated to improve visibility. Regions from the JHU WM atlases (sampled on the mean WM skeleton) demonstrating significant mean change are shown for FA (top), AD (middle), and RD (bottom). Regions in blue show significant increases, whereas ROIs in red depict regions demonstrating significant two-year decrease. B. Regions of interest (ROIs) showing significant individual differences in two-year latent change. The mean FA skeleton mask (white) is superimposed over the FMRIB58 1-mm FA image. Regions from the JHU WM atlases (sampled on the mean WM skeleton) demonstrating significant individual differences change are shown in green for FA (top), AD (middle), and RD (bottom). Skeletonized atlas regions were dilated to improve visibility.

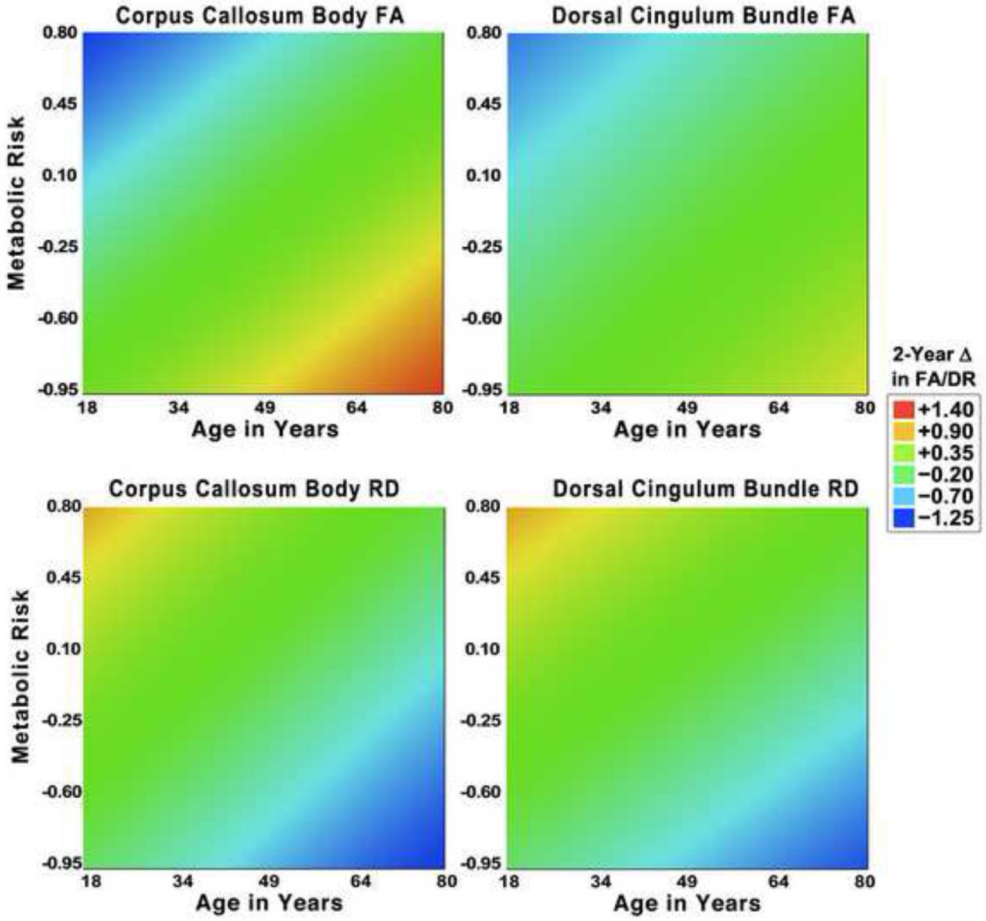

Figure 6.

Response surface plots depicting the relationship between baseline age, latent metabolic risk and latent two-year WM change. A linear smoother has been applied to each plot. All data are standardized to z-scores. Warm colors reflect two-year increases, and cool colors reflect longitudinal declines. Left: Corpus callosum; Right: Dorsal cingulum bundle. Top row: Fractional anisotropy; Bottom row: Radial diffusivity.

Table 1

Participant characteristics

	Women	Men		
Variable	**Mean (SD)**	**Mean (SD)**	***t* or χ^2**	***p***
Age (years)	54.59 (13.44)	55.3 (14.12)	−0.24	.814
Scan interval (months)	25.44 (2.13)	24.54 (2.12)	1.93	.056
MMSE	29.03 (0.99)	28.87 (0.97)	0.75	.453
Education (years)	15.73 (2.23)	15.47 (2.58)	0.51	.615
Systolic BP (mmHg)	120.24 (12.75)	125.41 (11.2)	−1.91	.059
Diastolic BP (mmHg)	73.86 (6.64)	77.81 (8.56)	−2.46	.016*
Fasting glucose (mg/dl)	87.23 (8.07)	91.93 (9.78)	−2.39	.020*
HDL (mg/dL)	60.68 (15.34)	45.69 (10.52)	4.78	.000*
LDL (mg/dL)	117.38 (34.67)	113.07 (33.82)	0.56	.575
Triglycerides (mg/dL)	105.96 (65.32)	133.83 (73.16)	−1.85	.068
Waist-to-Hip Ratio	0.83 (0.07)	0.95 (0.06)	−8.38	.000*
% Exercise	78.80%	83.30%	0.27	.604
Days Exercise / Week	3.17 (2.14)	3.83 (2.19)	−1.41	.163
% Hypertension Dx	15.15%	30.00%	4.13	.042*

Notes: SD=standard deviation; BP=blood pressure; HDL=high density lipoprotein; LDL=low density lipoprotein; Dx=diagnosis;

*=significant result.

Table 2

Univariate latent change score model results without covariates

	AD			RD			FA		
ROI	**Mean Δ**	***d***	**Δ Var.**	**Mean A**	***d***	**Δ Var.**	**Mean A**	***d***	**Δ Var.**
Association fibers									
CBd	−2.26*	−0.36	1.55	−1.75	−0.16	3.06*	0.41	0.05	3.44*
CBv	−6.96*	−1.15	1.77	−2.86*	−0.37	0.53	−0.40	−0.06	0.10
IFOF	−3.73*	−0.36	1.35	2.45*	0.13	2.83*	−3.57*	−0.26	2.96*
ILF	−4.14*	−0.43	–	–	0.00	0.43	−1.50	−0.18	1.16
SLF	−5.70*	−0.36	3.47*	−0.14	−0.01	2.49*	−1.27	−0.07	2.17
UF	−3.68*	−0.38	1.80	−1.48	−0.13	2.22*	−0.49	−0.04	2.30*
Commissural fibers									
CC genu	3.30*	0.50	1.40	4.93*	0.22	0.36	−3.29*	−0.16	0.49
CC body	0.53	0.06	4.12*	−4.71*	−0.30	5.77*	3.62*	0.33	4.88*
CC splenium	−1.96	−0.22	0.92	2.35*	0.15	2.11	−1.34	−0.12	1.58
FMajor	1.02	0.16	1.91	5.45*	0.34	0.48	−4.02*	−0.29	1.08
FMinor	2.22*	0.17	3.73*	5.52*	0.31	4.66*	−4.21*	−0.26	4.13*
Projection fibers									
ALIC	−4.78*	−0.34	2.53*	−	0.000	2.88*	−1.09	0.08	2.55*
PLIC	−7.00*	−0.75	0.51	−7.99*	−0.75	3.58*	3.28*	0.32	2.04

Notes: Mean Δ = latent mean change parameter as estimate/standard error; *d* = Cohen's *d;* Δ Var.= latent variance in change parameter as estimate/standard error; – = parameter constrained to zero;

* = significant following FDR correction

Table 3

Comparison of baseline age-DTI correlations and two-year mean change

	AD		RD		FA	
	***r*-age**	**Mean Δ**	***r*-age**	**Mean Δ**	***r*-age**	**Mean Δ**
CBd	−	−	+	−	−	Ø
CBv	Ø	−	Ø	−	Ø	Ø
IFOF	Ø °	−	+	+	−	−
ILF	Ø °	−	+	Ø	−	Ø
SLF	Ø °	−	+	Ø	−	Ø
UF	Ø	−	Ø	Ø	Ø	Ø
CC body	Ø °	Ø	+	−	−	+
CC genu	Ø °	+	+	+	−	−
CC splenium	Ø	−	+	Ø	−	Ø
FMajor	Ø	Ø	+	+	−	−
FMinor	−	+	+	+	−	−
ALIC	Ø	−	+	Ø	−	−
PLIC	Ø	−	+	−	−	+

Notes: Δ=two-year change; Ø = no significant effect; – = negative effect; + = positive effect; ° = relationship constrained to zero to improve fit

Table 4

Univariate model results without covariates – Normotensive participants only

	AD			RD			FA		
ROI	**Mean Δ**	***d***	**Δ Var.**	**Mean Δ**	***d***	**Δ Var.**	**Mean Δ**	***d***	**Δ Var.**
Association fibers									
CBd	−2.38*	−0.36	1.52	−1.11	−0.12	2.99*	−0.32	−0.04	3.32*
CBv	−4.79*	−1.15	1.07	−1.82	−0.28	0.80	−0.53	−0.13	–
IFOF	−2.71*	−0.36	1.23	2.88*	0.19	1.91	−3.30*	−0.28	2.90*
ILF	−2.91*	−0.43	0.88	0.36	0.04	–	−1.07	−0.17	1.06
SLF	−3.90*	−0.36	3.23*	−0.33	−0.02	1.88	−0.67	−0.04	1.62
UF	−2.08	−0.38	–	−1.50	−0.17	1.29	−0.04	−0.00	1.81
Commissural fibers									
CC genu	3.16*	0.50	1.16	4.62*	0.28	0.11	−2.90*	−0.19	0.15
CC body	–	0.06	3.32*	−3.27*	−0.24	5.24*	1.89	0.23	4.19*
CC splenium	−2.01	−0.22	0.35	2.41*	0.21	1.50	−2.97*	−0.26	1.78
FMajor	1.82	0.16	0.80	4.41*	0.35	0.19	−2.92*	−0.25	0.82
FMinor	2.77*	0.17	3.85*	5.06*	0.42	4.47*	−3.83*	−0.32	3.68*
Projection fibers									
ALIC	−3.91*	−0.34	1.61	−0.40	−0.027	1.89	−1.443	−0.12	2.10
PLIC	−6.55*	−0.75	0.80	−8.18*	−0.731	3.53*	3.695*	0.29	2.75*

Notes: Mean Δ = latent mean change parameter as estimate/standard error; *d* = Cohen's *d;* Δ Var.= latent variance in change parameter as estimate/standard error; – = parameter constrained to zero;

* = significant following FDR correction